Journal of Saudi Chemical Society (2015) **19**, 485–493

King Saud University

Journal of Saudi Chemical Society

www.ksu.edu.sa
www.sciencedirect.com

ORIGINAL ARTICLE

Photocatalytic degradation of 2,4-D and 2,4-DP herbicides on Pt/TiO_2 nanoparticles

M. Abdennouri [a], A. Elhalil [a], M. Farnane [a], H. Tounsadi [a], F.Z. Mahjoubi [a], R. Elmoubarki [a], M. Sadiq [a], L. Khamar [a], A. Galadi [b], M. Baâlala [c], M. Bensitel [c], Y. El hafiane [d], A. Smith [e], N. Barka [a,*]

[a] *Univ Hassan 1, Laboratoire des Sciences des Matériaux, des Milieux et de la Modélisation (LS3M), BP.145, 25000 Khouribga, Morocco*
[b] *Equipe de Recherche Analyse Contrôle et Environnement (ERACE), EST Safi, BP: 89, Route Dar Si Aissa, Safi, Morocco*
[c] *Laboratoire de Catalyse et Corrosion des Matériaux, Faculté des Sciences, Université Chouaib Doukkali, BP: 20, 24000 El Jadida, Morocco*
[d] *LMPEQ, ENSA Safi, Université Cadi Ayyad, Sidi Bouzid, B.P. 63, Safi 46000, Morocco*
[e] *GEMH, Ecole Nationale Supérieure de Céramique Industrielle, Centre Européen de la Céramique, 12 rue Atlantis, 87068 Limoges cedex, France*

Received 1 March 2015; revised 17 June 2015; accepted 20 June 2015
Available online 27 June 2015

KEYWORDS

Platinum supported TiO_2;
Photocatalysis;
Herbicides;
Water treatment

Abstract Titanium dioxide was synthesized by the sol–gel method and platinum supported on titanium dioxide were prepared by a wet impregnation chemical process at different platinum contents. The prepared samples were dried over night at 110 °C and then calcined at 500 °C for 4 h. Structural and morphological characterization has been carried out by means of X-ray diffraction (XRD), differential scanning calorimetry–thermogravimetric analysis (DSC–TGA), Raman spectroscopy, Fourier-transform infrared spectroscopy (FT-IR), Brunauer–Emmett–Teller surface area measurement (BET) and transmission electron microscopy coupled to the energy dispersive spectroscopy (TEM/EDX). The adsorption performance and photocatalytic activity of the samples were investigated using two chlorophenoxy herbicides: 2,4-dichlorophenoxyacetic acid (2,4-D) and 2-(2,4-dichlorophenoxy) propionic acid (2,4-DP) as models of organic pollutants in water. The obtained results show that Pt/TiO_2 exhibited higher photocatalytic activity than TiO_2 particles

* Corresponding author. Tel.: +212 661 66 66 22; fax: +212 523 49 03 54.
E-mail address: barkanoureddine@yahoo.fr (N. Barka).
Peer review under responsibility of King Saud University.

Production and hosting by Elsevier

http://dx.doi.org/10.1016/j.jscs.2015.06.007

for the degradation of the two selected herbicides. The photocatalytic activity increases by increasing the platinum yield in the catalyst.

1. Introduction

Titanium dioxide is a versatile material, which has been used in many applications such as photocatalytic degradation of organic compounds in water [1–3]. Several methods were adopted for the synthesis of titanium dioxide. The most conventional is sol–gel method from titanium alkoxides which depends entirely on precursors of departure [4–6]. Noble metal particles dispersed on TiO_2 surface have been investigated greatly for enhancing photocatalytic activities [7–11]. It has been reported that depositing some noble metals such as platinum and gold [12,13] on titania could inhibit the recombination of electron–hole pairs significantly and also result in the extension of their wavelength response toward the visible region. For the reasons given above the platinum loaded titanium dioxide which were prepared by a wet impregnation method have recently received considerable attention as promising candidates for many applications.

At present, several efforts have been made to convert the TiO_2 adsorption from the ultraviolet to the visible region by modification [14,15] or by doping with several transition metals, including, cerium [16], tungsten [17,18], molybdenum [19–22], gold [23], nickel [24–26] and platinum [27] ions. Other works have been directed toward modifying titanium dioxide and testing other semiconductors to identify ways to increase process efficiency and to improve the overlap of the absorption spectrum of the photocatalyst with the solar spectrum [28–32].

In the present work, we prepared a series of different platinum modified TiO_2 samples. The obtained photocatalysts were characterized by means of X-ray diffraction (XRD), differential scanning calorimetry–thermogravimetric analysis (DSC–TGA), Raman spectroscopy, Fourier-transform infrared spectroscopy (FT-IR), Brunauer–Emmett–Teller adsorption analysis (BET) and transmission electron microscopy (TEM) coupled to the energy dispersive spectroscopy (EDX). The samples were evaluated for the degradation of 2,4-D and 2,4-DP herbicides under UV irradiation. The increasing effects of photocatalytic activity were discussed.

2. Experimental methods

2.1. Materials

All of the reagents used in this work were of analytical grade and were used without any further purification: titanium tetraisopropoxide ($Ti(OC_3H_7)_4$, Fluka company, 98% purity) absolute ethanol (C_2H_6O, Prolalo, 99.85%), methanol (Prolalo, 97%), diethyl ether ($C_4H_{10}O_3$, Loba Chemie society), diamminedinitritoplatinum (II) solution ($Pt(NO_2)_2(NH_3)_2$, Sigma–Aldrich), 2,4-dichlorophenoxyacetic acid (2,4-D) ($C_8H_6Cl_2O_3$, Fluka company, 95% purity) and 2,4-dichlorophenoxypropionic acid (2,4-DP) ($C_9H_8Cl_2O_3$, Sigma–Aldrich Chemical Company, 95% purity). Characteristics and molecular structures of 2,4-D and 2,4-DP were displayed in Table 1. The solutions were prepared by using pure distilled water obtained from a Millipore Milli-Q laboratory system.

2.2. Preparation of photocatalysts x%-Pt/TiO_2

The TiO_2 used in this study as prepared by the sol–gel method by dissolving $Ti(OC_3H_7)_4$ in methanol/ethanol solution with molar ratio 1:1:10 respectively. The obtained solution was maintained at 75 °C for 3 h and the appropriate amount of water was added drop wise into the hot solution. After gelling, the sample was separated by filtration. The obtained solid was dried at 110 °C during a night in the steam room then calcined in 500 °C for 4 h. x%-Pt/TiO_2 samples were prepared by a standard wet impregnation method. To impregnate Pt, the appropriate quantity of diamminedinitrito platinum solution was added on the dried TiO_2 support. The obtained mixtures were then dried and calcined as described above. The amount of platinum loading was varied from 0.5 to 3 weight%.

Table 1 Physicochemical properties of 2,4-D and of 2,4-DP herbicides.

Herbicides	Chemical formula	MW (g/mol)	λ_{max} (nm)
2,4-Dichlorophenoxyacetic acid (2,4-D)	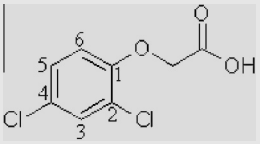	221.04	283
2-(2,4-Dichlorophenoxy) propionic acid (2,4-DP)	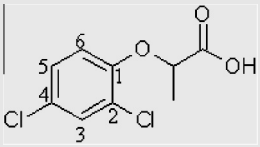	235.06	284

2.3. Characterization

Crystalline phases present in the photocatalysts were determined by X-ray diffraction method. The pattern was scanned from 2θ of 20–80° at a scan rate of 2°/min using a diffractometer X'Pert High Score type with Cu Kα radiation. The accelerating voltage and the applied current were 40 kV and 35 mA, respectively. The thermal analyses are made with the device SESTYS 24. It allows realizing simultaneously differential thermal analysis (ATD) and thermogravimetric analysis (ATG) behavior of the as-prepared samples under air atmosphere in the temperature range 25–800 °C and with heating rate of 5 °C/min. Raman spectra were recorded at room temperature using a Raman microprobe (infinity from Jobin–Yvon) in the range of 700–200 cm^{-1} with a spectral resolution of 2 cm^{-1}. The exciting laser source was the 532.16 nm line with a laser power of 600 mW of a diode pumped Nd-YAG laser (899.92 cm^{-1}) and a super InGaAs as detector. FT-IR absorption spectra were measured by Nicolet MX 710 spectrophotometer in the region of 4000–400 cm^{-1}. Specific surface area measurements were carried out by N_2 adsorption at −196 °C using a Micromeritics Instrument TriStar II 3020. The structure of TiO_2 and platinum loaded titanium dioxide catalysts was observed using transmission electron microscopy (TEM) with a JEM-2010F microscope (JEOL) at an acceleration voltage of 200 kV. Elemental analysis of the catalyst was performed using an energy dispersive X-ray spectrometer (EDS: Noran) attached to the JEM-2010F.

2.4. Photocatalytic experiments

Photocatalytic experiments were performed in a cylindrical quartz glass batch reactor with 10 cm in diameter and 20 cm in height as descried in our previous work [33]. Irradiation was performed with a medium pressure mercury-lamp (400 W), placed in axial position inside a cooling water jacket system. The wavelength of maximum of the light source of the lamp is 365 nm. Constant agitation was assured by means of a magnetic stirrer placed at the reactor base. The reactor was initially loaded with 800 ml of 2,4-D or 2,4-DP aqueous solution at 20 mg/L and 120 mg of the photocatalyst. The mixture was maintained in the dark for 30 min under stirring to reach adsorption equilibrium, and was then irradiated. Samples taken at different time intervals were centrifuged at 3000 tr/min for 10 min. The residual concentration was determined from UV–Vis absorption characteristic with the calibration curve method at the wavelength of maximum absorption of 283 and 284 nm, respectively, for 2,4-D and 2,4-DP. A GBC UV/Vis 911 spectrophotometer was used.

3. Results and discussion

3.1. Characterization of photocatalysts

Catalyst characterization was carried out to identify the correlation between the catalysts structures and their photocatalytic activity. Different characterization techniques used in this work are described below.

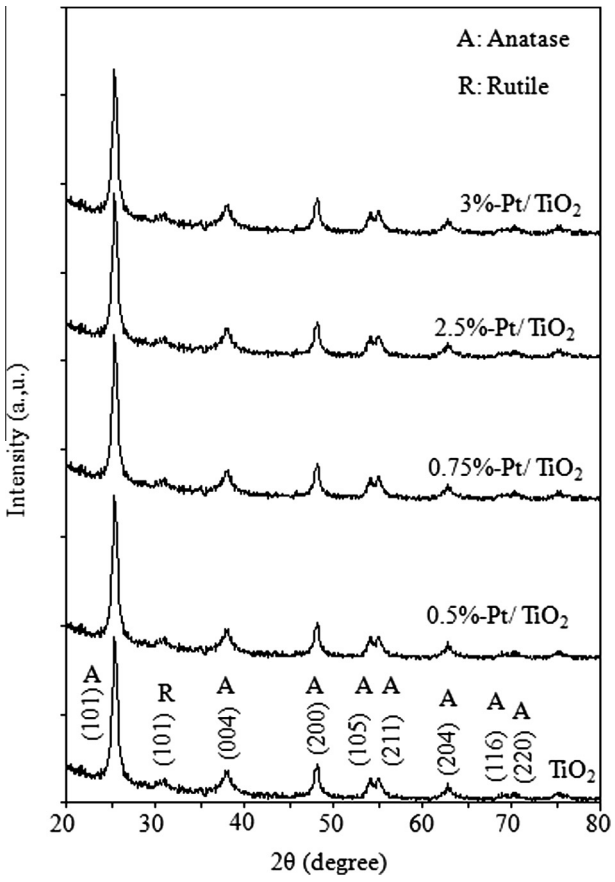

Figure 1 X-ray diffraction patterns of TiO_2 and x%-Pt/TiO_2 samples.

3.1.1. X-ray diffraction (XRD)

Fig. 1 shows the X-ray diffraction pattern of the samples. The XRD of prepared TiO_2 reveals diffraction peaks characteristic corresponding to (101), (004), (200), (105), (211), (104), (216) and (215) reticular plane of anatase phase. A weak peak at $2\theta = 31.6°$ was attributed to the (103) reticular plane of rutile phase. The fineness peaks indicated that the nanosized materials were well crystallized. The X-ray diffraction patterns of x%-Pt/TiO_2 samples are well crystallized. Their indexation shows that their peaks similar are to those identified on as-synthesized TiO_2. On the one hand, the addition of the platinum within the limits of detection of the device and the percentage loaded amount of platinum nanoparticles on the TiO_2 powder, showed the absence of change of the structure of departure. On the other hand, no new phase was detected. The absence of additional diffractions in x%-Pt/TiO_2 samples indicated that platinum was highly dispersed throughout the surface of TiO_2, as was previously reported by Kim et al. [34] and by Sakthivel et al. [35,7].

3.1.2. DSC–TGA analysis

Fig. 2 shows the TGA–DSC patterns of the samples. As shown in the figure, TGA analysis of pure titania shows a total weight loss of 13.80%. The loss of mass observed around 200 °C is due to the removal of loosely bound water of the sample. The decomposition step between 220 and 400 °C is due to

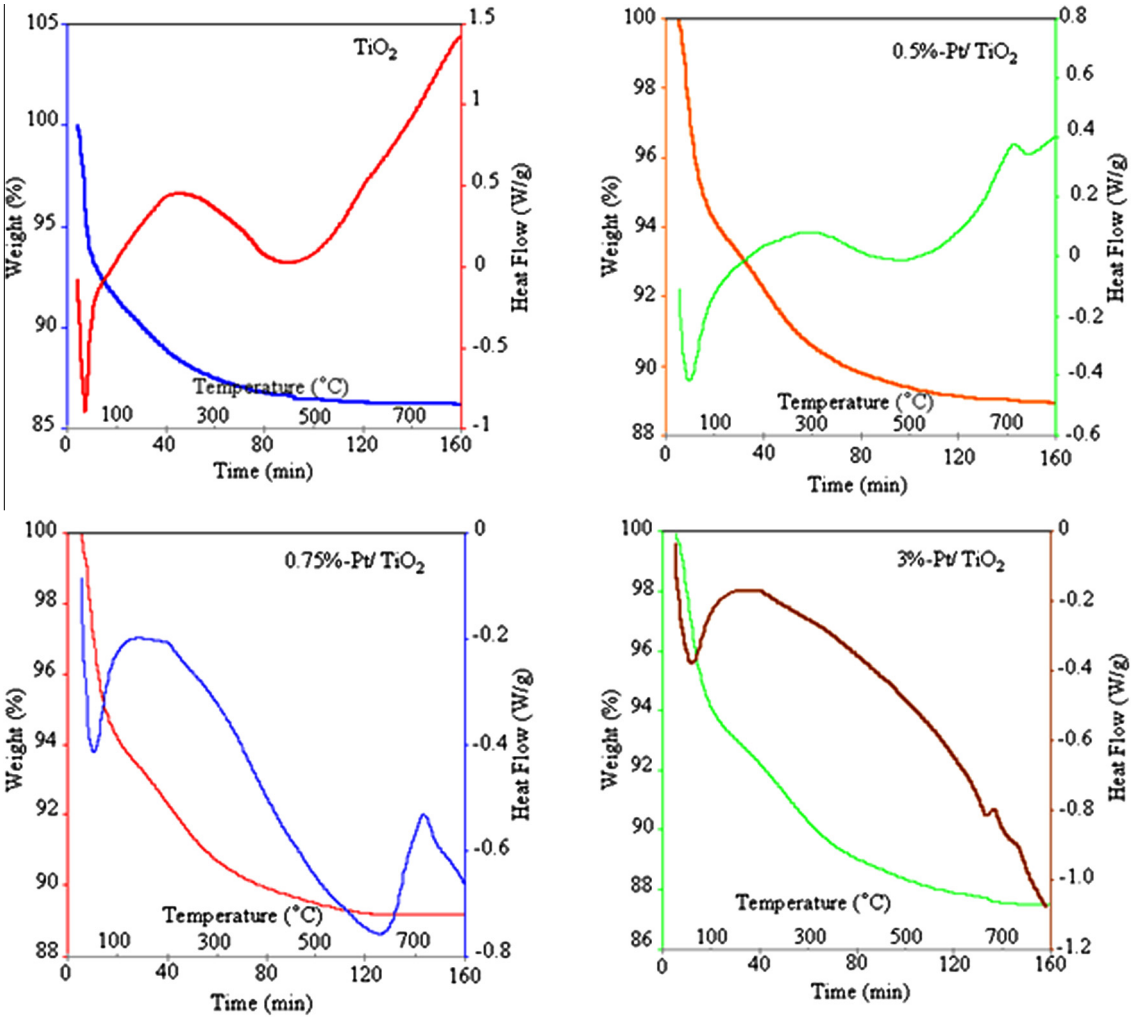

Figure 2 TGA–DSC analysis of the samples.

the dehydroxylation of the sample. Beyond 400 °C the loss of mass becomes low. The result of the DSC analysis is complementary to the results of the TGA which shows that the wide exothermic band centered on 200 °C attributed to the dehydroxylation of the samples.

TGA analysis of the x%-Pt/TiO_2 samples shows a total mass loss between 11.07 and 13.44%. A mass loss of 5% appears in the range of 100–200 °C, which corresponds to the removal of the adsorbed water and which may include the evaporation of excess ethanol and methanol. The decomposition step between 200 and 420 °C is due to the decomposition of nitrate ions and dehydroxylation of the samples. In the same way, the DSC pattern shows a small large band centered around 300 °C, which is attributed to the decomposition of nitrates species and an extremely small exothermal peak, centered around 740 °C, indicating the slow anatase to rutile transformation in these prepared samples.

3.1.3. Raman spectra

The Raman spectra of TiO_2 and platinum loaded TiO_2 catalysts are illustrated in Fig. 3. The figure shows the Raman spectra of prepared TiO_2 reveals peaks at 488, 408 and 325 cm^{-1} attributed to the anatase phase of titanium dioxide while no absorption peaks attributed to the rutile phase were observed. The Raman patterns of platinum doped TiO_2 samples almost coincide with those of pure TiO_2 and show no absorption peaks due to platinum species. But, the observed difference was the intensive decrease of the peaks at 488 and 325 cm^{-1} as the amount of platinum loading on the photocatalyst support increased. This can be explained by the interaction between titanium and platinum in substitution sites. The results obtained from the Raman analysis were in perfect correlation with those found by the X-ray diffraction.

3.1.4. FT-IR analysis

Fig. 4 shows FT-IR spectra of synthesized TiO_2 and platinum loading titanium dioxide samples recorded at room temperature in a spectral domain were between 4000 and 400 cm^{-1}. Anatase phase of titania exhibits strong absorption bands at 640 cm^{-1}, this peak is for O–Ti–O bonding vibration. No rutile phase peak is detected in this experiment, because the instrument employed is weak. The presence of these bands due to TiO_2 anatase phase is noted for both samples limited. Generally, the bands situated at 3401 cm^{-1} and at 1632 cm^{-1}, are attributed to the stretching

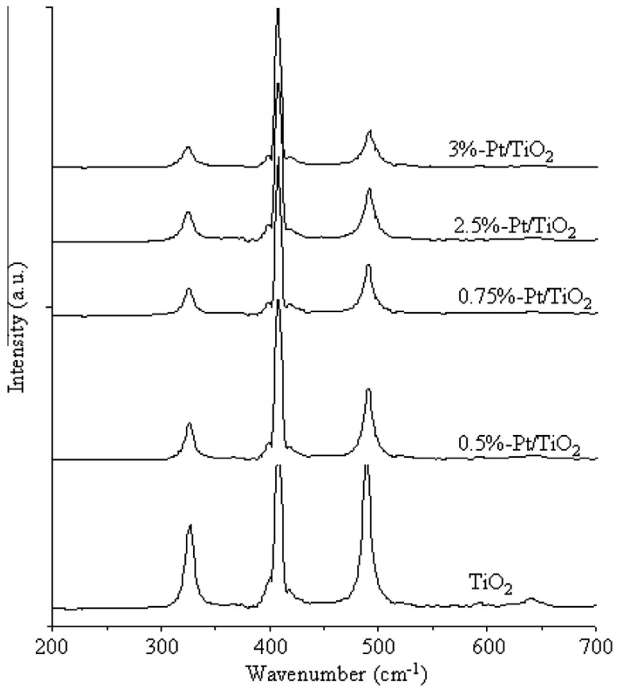

Figure 3 Raman spectra of calcined samples at 500 °C.

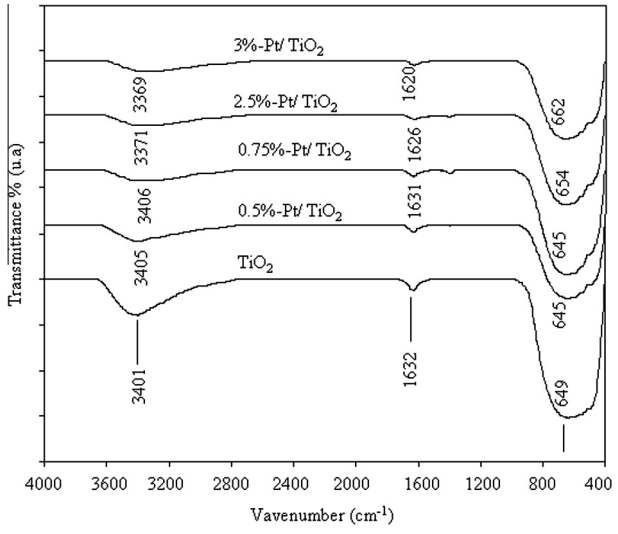

Figure 4 FT-IR spectra of the samples calcined at 500 °C.

and bending of hydroxyls vibrations of the Ti-OH groups, respectively [36,37]. The bands situated in the region 800–400 cm^{-1} are assigned to the stretching vibration modes characteristic of Ti–OH and Ti–O–Ti bonds [38–40]. The vibration band at 640 cm^{-1} is generally attributed to the deformation mode of the M–OH bond (M = metal). In the samples Pt/TiO_2, no characteristic bands due to the crystalline PtO_2 were observed which indicates clearly that the platinum oxide is highly dispersed on the pure titania or these metal sites are expected to be below the visibility limit of FT-IR analysis.

Table 2 BET surface area of TiO_2 and x%-Pt/TiO_2 samples.

Catalysts samples	BET surface area (m^2/g)
TiO_2	67.66
0.5%-Pt/TiO_2	79.81
0.75%-Pt/TiO_2	86.65
2.5%-Pt/TiO_2	97.21
3%-Pt/TiO_2	108.24

3.1.5. Specific surface area determination

The values of the specific surface area samples calculated from the classic formula of Brunauer–Emmet–Teller are summarized in Table 2. The BET specific surface area of TiO_2 is estimated to be 67.66 m^2/g. After impregnation with platinum, a significant increase was noticed in the specific surface area of the samples Pt/TiO_2. As the platinum load increases, the surface areas increases.

3.1.6. TEM morphology

TEM and EDX were used to study the morphologies and elemental distribution of the samples. Fig. 5 illustrates TEM micrographs and EDX patterns of TiO_2, 0.5%-Pt/TiO_2 and 3%-Pt/TiO_2. The figure clearly showed that all the samples were nanometric in crystalline size. The particles exhibit an irregular distribution. The morphology of platinum loaded on TiO_2 powders is almost the same because the doping amount is small. The platinum possesses a covalent radius of 1.30 Å and ray to states Pt^{2+} and Pt^{4+} respectively of the order of 0.80 Å and 0.65 Å. The titanium in the state Ti^{4+} possesses an ionic radius of the order of 0.68 Å. Consequently, the ion Pt^{4+} can be easily inserted inside the titanium dioxide structure. In particular, the insertion of the ions Pt^{4+} is made without distortion of the photocatalyst structure. The elemental analysis shown in energy dispersive X-ray spectra of TiO_2 reveals the presence of Ti and O peaks without any other impurity. EDX patterns of 0.5%-Pt/TiO_2 and 3%-Pt/TiO_2 show Pt peaks along with Ti and O which confirms the doping of Pt in TiO_2.

3.2. Photocatalytic activity

3.2.1. Photolytic degradation

The photocatalytic performance of each prepared samples was tested for the degradation of 2,4-D and 2,4-DP photo reaction in an aqueous solution. In the same operating conditions for the photocatalytic degradation, the photolytic degradation was studied using 800 ml of 2,4-D or 2,4-DP at 20 mg/L. The solution was irradiated without photocatalysts. The results are illustrated in Figs. 6 and 7. Kinetics of pesticides photolytic degradation shows that, after 90 min of irradiation, a very low diminution of the concentration was observed. According to this result, we can neglect the interference of the photolytic degradation with the photocatalytic degradation.

3.2.2. Photocatalytic behavior

To test the photodegradability of 2,4-D and 2,4-DP on the prepared photocatalysts under ultraviolet–visible light irradiation, a series of experiments were performed according to the similar procedure described above. From Figs. 6 and 7, it can be seen

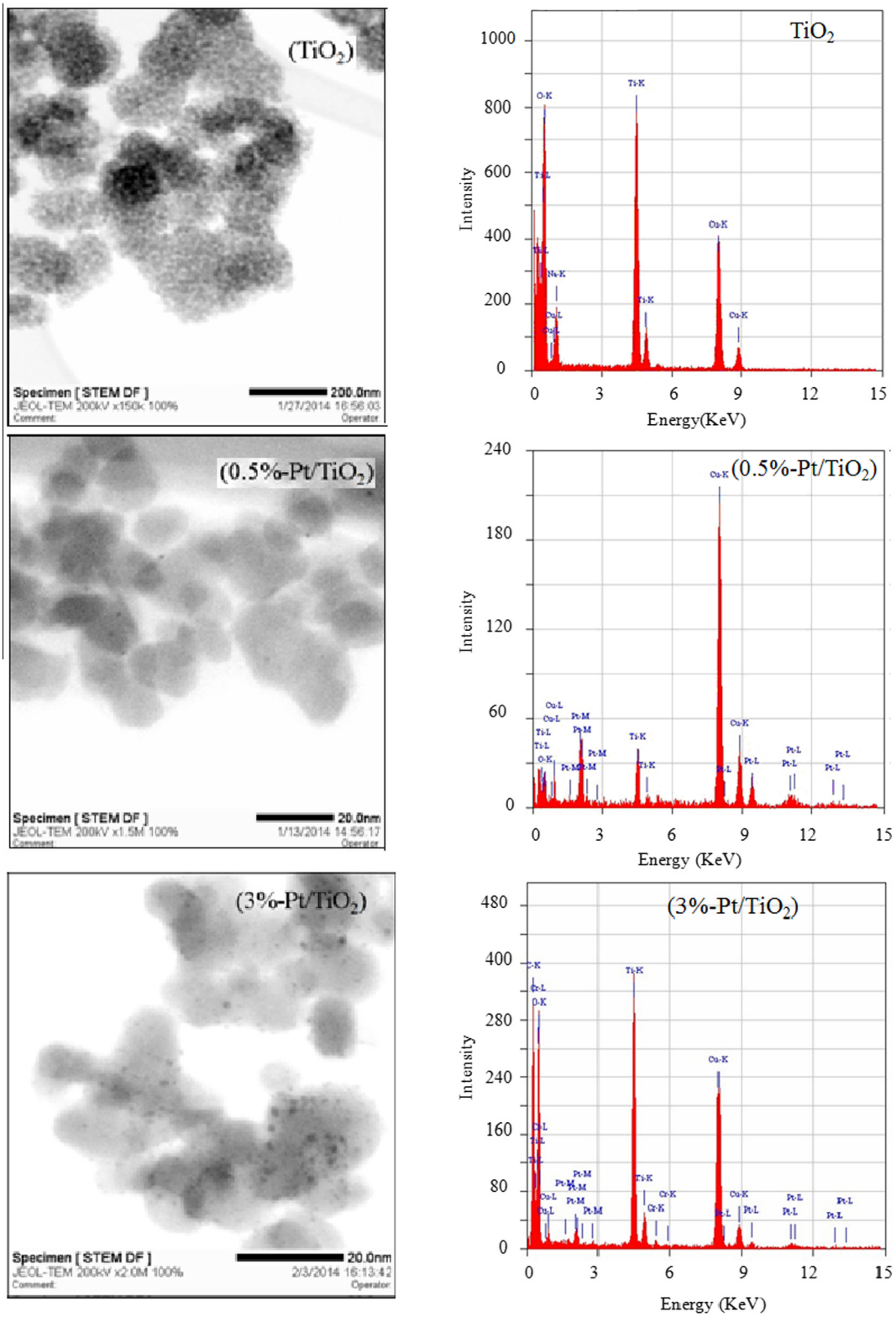

Figure 5 TEM micrographs and EDX patterns of TiO_2, 0.5%-Pt/TiO_2 and 3%-Pt/TiO_2.

that the addition of TiO_2 strongly enhances the degradation of 2,4-D and 2,4-DP. The illumination of TiO_2 by UV light ($\lambda \leqslant 390$ nm), changes the energy state of electrons from the valence band to the conduction band to give electron–hole pairs. The holes at the TiO_2 valence band can oxidize water or hydroxide to produce hydroxyl radicals. The hydroxyl radical is a powerful oxidizing agent and attacks organic compounds and intermediates (Int) are formed. These intermediates react with hydroxyl radicals to produce final products (CO_2, H_2O and mineral salts):

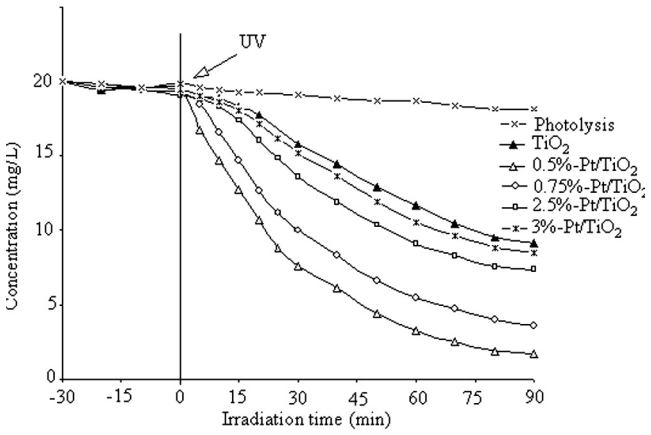

Figure 6 Variation of 2,4-D concentration versus irradiation time without and with the photocatalysts.

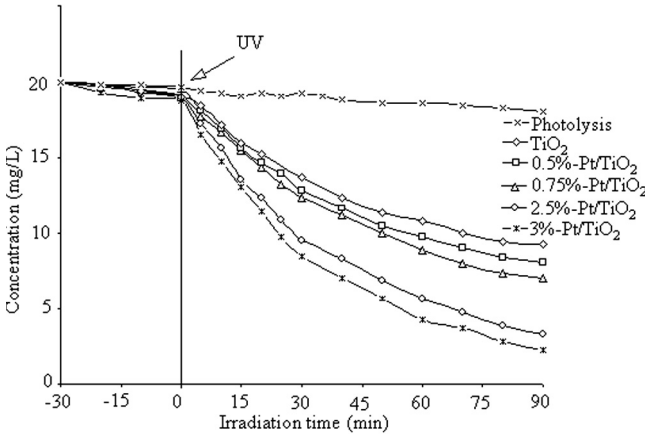

Figure 7 Variation of 2,4-DP concentration versus irradiation time without and with the photocatalysts.

$$TiO_2 + h\upsilon \longrightarrow e^- + h^+ \quad (1)$$

$$h^+ + H_2O_{ads} \longrightarrow {}^{\cdot}OH_{ads} + H^+ \quad (2)$$

$$h^+ + OH^-_{ads} \longrightarrow {}^{\cdot}OH_{ads} \quad (3)$$

$${}^{\cdot}OH_{ads} + (2,4D \text{ or } 2,4DP)_{ads} \longrightarrow Int \quad (4)$$

$${}^{\cdot}OH_{ads} + Int \longrightarrow CO_2 + H_2O + HCl \quad (5)$$

The photocatalytic activities of platinum loaded on titanium oxide samples were higher than that of titanium dioxide support photocatalyst. A possible explanation is that the catalytic activity order is mainly attributed to the bad gap energy reduction, long-term life of electron (e^-)/hole (h^+) during catalyst semiconductor illumination under ultra violet light. The band gap of PtO_2 is 2.5 eV, which corresponds to absorption out to approximately 500 nm, in the visible region. Moreover, because of the absolute positions of the bands, conduction bond electrons from TiO_2 can migrate to PtO_2, while the complementary migration can occur for valence band holes. A similar observation has also been reported by Hathway et al. [41]. However, this observation showed that the highest catalytic activity is due in a large part to the extended near-visible absorption of the anatase phase, followed by a rapid electron transfer between the phases, leading to enhanced charge separation and reduced energy wastage by electron–hole recombination.

It can be seen from the figures that in the presence of x%-Pt/TiO_2 samples, the degradation rate increased with the increase of platinum loading. The experimental results indicated that high mass ratio of platinum shows the highest catalytic activity among all the compositions investigated. The order of catalytic activity for 2,4-D and 2,4-DP was 3%-Pt/TiO_2 > 2.5%-Pt/TiO_2 > 1.5%-Pt/TiO_2 > 0.75%-Pt/TiO_2 > 0.5%-Pt/TiO_2 > TiO_2.

The relation between amount of Pt in the catalyst and the photocatalytic degradation rate can be explained by the fact that Pt acts as an electron trap. The electrons generated on the TiO_2 surface by UV light illumination quickly move to Pt particle to facilitate the effective separation of the photogenerated electron and holes, resulting in the significant enhancement of photocatalytic activity [42]. Pt plays a positive role as electron acceptor, more acceptor centers are provided with increasing Pt-doping, therefore the degradation rate for 2,4-D and 2,4-DP increases with the increase of Pt content.

4. Conclusions

Titanium dioxide and platinum loaded on titanium dioxide were successfully synthesized by the sol–gel process. X-ray powder diffraction, differential scanning calorimetry–thermogravimetric analysis (DSC–TGA), Raman spectroscopy, FT-IR spectroscopy, Nitrogen adsorption–desorption and transmission electron microscopy confirmed the formation of good quality crystalline nanomaterials. The photocatalytic activity remained high at 3%-Pt/TiO_2. For each prepared Pt/TiO_2, anatase was still the major phase. The x%-Pt/TiO_2 catalysts calcined at 500 °C also retain the TiO_2-anatase phase of the support and the impregnated metallic oxide being in a highly dispersed state. A perfect match was found between the platinum amounts loading in the catalyst and the efficiency photocatalytic degradation reaction of 2,4-D and 2,4-DP. Finally, we conclude that all the doped prepared samples exhibited better catalytic performance than the unmodified TiO_2 sample, for the two selected herbicides used in this study. This enhanced photocatalytic activity can be attributed to the crystallinity, nanosize, large amount of surface hydroxyl species, reduced band-gap and retard the fast charge pair recombination.

References

[1] A. Abaamrane, S. Qourzal, M. El Ouardi, S. Alahiane, M. Belmouden, H. Bari, N. Barka, S. Mançour Billah, A. Assabbane, Y. Ait-Ichou, Modeling of photocatalytic mineralization of phthalic acid in TiO_2 suspension using response surface methodology (RSM), Desal. Water Treat. 53 (1) (2015) 249–256.

[2] N. Barka, I. Bakas, S. Qourzal, A. Assabbane, Y. Ait-Ichou, Degradation of phenol in water by titanium dioxide photocatalysis, Orient. J. Chem. 29 (3) (2013) 1055–1060.

[3] S. Qourzal, N. Barka, M. Belmouden, A. Abaamrane, S. Alahiane, M. Elouardi, A. Assabbane, Y. Ait-Ichou, Heterogeneous photocatalytic degradation of 4-nitrophenol on

suspended titania surface in a dynamic photoreactor, Fresenius Environ. Bull. 21 (7) (2012) 1972–1981.
[4] M.R. Bayati, F. Golestani-Fard, A.Z. Moshfegh, Visible photodecomposition of methylene blue over micro arc oxidized WO_3-loaded TiO_2 nano-porous layers, Appl. Catal. A Gen. 382 (2010) 322–331.
[5] H. Lin, C.P. Huang, W. Li, C. Ni, S. Ismat Shah, Yao-Hsuan Tseng, Size dependency of nanocrystalline TiO_2 on its optical property and photocatalytic reactivity exemplified by 2-chlorophenol, Appl. Catal. B Environ. 68 (2006) 1–11.
[6] N. Barka, S. Qourzal, A. Assabbane, A. Nounah, Y. Ait-Ichou, Triphenylmethane dye, patent blue V, photocatalytic degradation on supported TiO_2: kinetics, mineralization and reaction pathway, Chem. Eng. Commun. 198 (2011) 1233–1243.
[7] L. Ravichandran, K. Selvam, B. Krishnakumar, M. Swaminathan, Photovalorisation of pentafluorobenzoic acid with platinum doped TiO_2, J. Hazard. Mater. 167 (2009) 763–769.
[8] A. Sclafani, J.M. Herrmann, Influence of metallic silver and of platinum-silver bimetallic deposits on the photocatalytic activity of titania (anatase and rutile) in organic and aqueous media, J. Photochem. Photobiol. A Chem. 113 (1998) 181–188.
[9] A. Wold, Photocatalytic properties of titanium dioxide (TiO_2), Chem. Mater. 5 (1993) 280–283.
[10] V. Subramanian, E. Wolf, P. Kamat, Semiconductor-metal composite nanostructures to what extent do metal nanoparticles improve the photocatalytic activity of TiO_2 films, J. Phys. Chem. B 105 (2001) 11439–11446.
[11] C.Y. Wang, C.Y. Liu, X. Zheng, J. Chen, T. Shen, The surface chemistry of hybrid nanometer-sized particles I. Photochemical deposition of gold on ultrafine TiO2 particles, Colloid Surf. A 131 (1998) 271–280.
[12] H. Kim, Y. Choi, N. Kanuka, H. Kinoshita, T. Nishiyama, T. Usami, Preparation of Pt-loaded TiO_2 nanofibers by electrospinning and their application for WGS reactions, Appl. Catal. A Gen. 352 (2009) 265–270.
[13] F. Boccuzzi, A. Chiorino, M. Manzoli, D. Andreeva, T. Tabakova, L. Ilieva, V. Iadakiev, Gold, silver and copper catalysts supported on TiO_2 for pure hydrogen production, Catal. Today 75 (2002) 169–175.
[14] S. Kalathil, M. Mansoob Khan, S.A. Ansari, J. Lee, M.H. Cho, Band gap narrowing of titanium dioxide (TiO2) nanocrystals by electrochemically active biofilms and their visible light activity, Nanoscale 5 (2013) 6323–6326.
[15] M. Mansoob Khan, S.A. Ansari, D. Pradhan, M. Omaish Ansari, D.H. Han, J. Lee, M.H. Cho, Band gap engineered TiO2 nanoparticles for visible light induced photoelectrochemical and photocatalytic studies, J. Mater. Chem. A 2 (2014) 637–644.
[16] M. Mokhtar Mohamed, Effect of ceria-doped titania on the structure and acidic properties of MoO_3/TiO_2 catalysts, Appl. Catal. A Gen. 267 (2004) 135–142.
[17] M. Abdennouri, R. Elmoubarki, A. Elmhammedi, A. Galadi, M. Baâlala, M. Bensitel, A. Boussaoud, Y. El hafiane, A. Smith, N. Barka, Influence of tungsten on the anatase-rutile phase transition of sol–gel synthesized TiO_2 and on its activity in the photocatalytic degradation of pesticides, J. Mater. Environ. Sci. 4 (6) (2013) 953–960.
[18] E. Gyorgy, E. Axente, I.N. Mihailescu, C. Ducu, H. Duc, Doped thin metal oxide films for catalytic gas sensors, Appl. Surf. Sci. 252 (2006) 4578–4581.
[19] K. Karthik, S. Kesava Pandian, N. Victor Jaya, Effect of nickel doping on structural, optical and electrical properties of TiO_2 nanoparticles by sol–gel method, Appl. Surf. Sci. 256 (2010) 6829–6833.
[20] H.-H. Tseng, M.-C. Wei, S.-F. Hsiunga, C.-W. Chioua, Degradation of xylene vapor over Ni-doped TiO_2 photocatalysts prepared by polyol-mediated synthesis, Chem. Eng. J. 150 (2009) 160–167.
[21] L. Gomathi Devi, B. Narasimha Murthy, S. Girish Kumar, Heterogeneous photo catalytic degradation of anionic and cationic dyes over TiO_2 and TiO_2 doped with Mo^{6+} ions under solar light: correlation of dye structure and its adsorptive tendency on the degradation rate, Chemosphere 76 (2009) 1163–1166.
[22] Y. Du, Y. Gan, P. Yang, Z. Cuie, N. Hua, Cyclic voltammetry and contact angle measurement studies of the Mo(VI) ions doped TiO_2 thin films Materials, Chem. Phys. 103 (2007) 446–449.
[23] M. Mansoob, J. Khan, M.H. Lee Cho, Au@TiO_2 nanocomposites for the catalytic degradation of methyl orange and methylene blue: an electron relay effect, J. Ind. Eng. Chem. 20 (2014) 1584–1590.
[24] Y. Ishibai, J. Sato, S. Akita, T. Nishikawa, S. Miyagishi, Photocatalytic oxidation of NO_x by Pt-modified TiO_2 under visible light irradiation, J. Photochem. Photobiol. A Chem. 188 (2007) 106–111.
[25] Y. Murakami, I. Ohta, T. Hirakawa, Y. Nosaka, Direct detection of OH radicals in the gas-phase diffused from the Pt/TiO_2 and WO_3/TiO_2 photocatalysts under the UV-light irradiation, Chem. Phys. Lett. 493 (2010) 292–295.
[26] U.G. Akpan, B.H. Hameed, The advancements in sol–gel method of doped-TiO_2 photocatalysts, Appl. Catal. A Gen. 375 (2010) 1–11.
[27] S.A. Ansari, M. Mansoob Khan, M.O. Ansari, M.H. Cho, Improved electrode performance in microbial fuel cells and the enhanced visible light-induced photoelectrochemical behaviour of PtOx@m-TiO_2 nanocomposites, Ceram. Int. 41 (2015) 9131–9139.
[28] R. Saravanan, V.K. Gupta, V. Narayanan, A. Stephen, Visible light degradation of textile effluent using novel catalyst ZnO/γ-Mn_2O_3, J. Taiwan Inst. Chem. Eng. 45 (2014) 1910–1917.
[29] R. Saravanan, M. Mansoob Khan, V.K. Gupta, E. Mosquera, F. Gracia, V. Narayanan, A. Stephen, ZnO/Ag/CdO nanocomposite for visible light-induced photocatalytic degradation of industrial textile effluents, J. Colloid Interface Sci. 452 (2015) 126–133.
[30] R. Saravanan, V.K. Gupta, T. Prakash, V. Narayanan, A. Stephen, Synthesis, characterization and photocatalytic activity of novel Hg doped ZnO nanorods prepared by thermal decomposition method, J. Mol. Liq. 178 (2013) 88–93.
[31] R. Saravanan, S. Karthikeyan, V.K. Gupta, G. Sekaran, V. Narayanan, A. Stephen, Enhanced photocatalytic activity of ZnO/CuO nanocomposite for the degradation of textile dye on visible light illumination, Mater. Sci. Eng. C 33 (2013) 91–98.
[32] R. Saravanan, M. Mansoob Khan, V.K. Gupta, E. Mosquera, F. Gracia, V. Narayanan, A. Stephen, ZnO/Ag/Mn_2O_3 nanocomposite for visible light-induced industrial textile effluent degradation, uric acid and ascorbic acid sensing and antimicrobial activity, RSC Adv. 5 (2015) 34645–34651.
[33] N. Barka, M. Abdennouri, A. Boussaoud, A. Galadi, M. Baâlala, M. Bensitel, A. Sahibed-Dine, K. Nohair, M. Sadiq, Full factorial experimental design applied to oxalic acid photocatalytic degradation in TiO_2 aqueous solution, Arab. J. Chem. 7 (2014) 752–757.
[34] S.H. Kim, C.-H. Jung, N. Sahub, D. Park, J.Y. Yun, H. Ha, J.Y. Park, Catalytic activity of Au/TiO_2 and Pt/TiO_2 nanocatalysts prepared with arc plasma deposition under CO oxidation, Appl. Catal. A Gen. 454 (2013) 53–58.
[35] S. Sakthivel, M.V. Shankar, M. Palanichamy, B. Arabindoo, D.W. Bahnemann, V. Murugesan, Enhancement of photocatalytic activity by metal deposition: characterization and photonic efficiency of Pt, Au and Pd deposited on TiO_2 catalyst, Water Res. 38 (2004) 3001–3008.
[36] Saepurahman, M.A. Abdullah, F.K. Chong, Preparation and characterization of tungsten-loaded titanium dioxide

photocatalyst for enhanced dye degradation, J. Hazard. Mater. 176 (2010) 451–458.
[37] T. Bezrodna, G. Puchkovska, V. Shymanovska, J. Baran, H. Ratajczak, IR-analysis of H-bonded H_2O on the pure TiO_2 surface, J. Mol. Struct. 700 (2004) 175–181.
[38] Y.-F. Chena, C.-Y. Leec, M.-Y. Yeng, H.-T. Chiu, The effect of calcination temperature on the crystallinity of TiO_2 nanopowders, J. Cryst. Growth 247 (2003) 363–370.
[39] M. Ivanda, S. Musić, S. Popović, M. Gotić, XRD, Raman and FT-IR spectroscopic observations of nanosized TiO_2 synthesized by the sol-gel method based on an esterification reaction, J. Mol. Struct. 480–481 (1999) 645–649.
[40] K.M.S. Khalil, T. Baird, M.I. Zaki, A.A. El-Samahy, A.M. Awad, Synthesis and characterization of catalytic titanias via hydrolysis of titanium(IV) isopropoxide, Colloids Surf. A Physicochem. Eng. Aspects 132 (1998) 31–44.
[41] T. Hathway, E.M. Rockafellow, Y.-C. Oh, W.S. Jenks, Photocatalytic degradation using tungsten-modified TiO_2 and visible light: kinetic and mechanistic effects using multiple catalyst doping strategies, J. Photochem. Photobiol. A Chem. 207 (2009) 197–203.
[42] M. Anpo, M. Takeuchi, The design and development of highly reactive titanium oxide photocatalysts operating under visible light irradiation, J. Catal. 216 (2003) 505–516.